

Field activities of the “Snow Impurity and Glacial Microbe effects on abrupt warming in the Arctic” (SIGMA) Project in Greenland in 2011–2013

Teruo AOKI^{1*}, Sumito MATOBA², Jun UETAKE^{3, 4}, Nozomu TAKEUCHI⁵ and
Hideaki MOTOYAMA³

¹ Meteorological Research Institute, Tsukuba 305-0052, Japan

* teaoki@mri-jma.go.jp

² Institute of Low Temperature Science, Hokkaido University, Sapporo 060-0819, Japan

³ National Institute of Polar Research, Tachikawa, Tokyo 190-8518, Japan

⁴ Transdisciplinary Research Integration Center, Tokyo 105-0001, Japan

⁵ Department of Earth Sciences, Graduate School of Science, Chiba University, Chiba 263-8522, Japan

(Received April 4, 2014; Revised manuscript accepted May 23, 2014)

Abstract

Field activities of the “Snow Impurity and Glacial Microbe effects on abrupt warming in the Arctic” (SIGMA) Project in Greenland in the summer season of 2011–2013 are reported; this consists of (1) glaciological and meteorological observations and (2) biological observations. In 2011, we conducted a field reconnaissance in the Qaanaaq, Ilulissat and Kangerlussuaq areas to enable continuous meteorological observations with automatic weather stations (AWS), campaign observations for glaciology, meteorology and Biology and shallow ice core drilling, which were planned for 2012–2014. Based on the results, we chose the Qaanaaq area in northwest Greenland as our main activity area and the Kangerlussuaq area in mid-west Greenland partly for biological observations. In 2012, we conducted field observations for (1) and (2) mentioned above together with installations of two AWSs at site SIGMA-A on The Greenland ice sheet (GrIS) and at site SIGMA-B on the Qaanaaq ice cap (QIC) from June to August. Surface snow and ice over all of the QIC melted in July and August 2012, and most of the Glacier surface appeared to be dark-colored, probably due to mineral dust and glacial microbial products. In 2013, we carried out similar observations in the Qaanaaq area. However, the weather and Glacier surface conditions were considerably different from those in 2012. Snow cover over the summer of 2013 remained over large areas with elevations higher than about 700 m on QIC. Biological activity on the Glacier surface appears to be substantially lower as compared to that in 2012.

Key words: SIGMA, Greenland, Qaanaaq, snow impurities, glacial microbes

1. Introduction

Snow surface albedo depends strongly on snow grain size and mass concentration of light-absorbing snow impurities (Warren and Wiscombe, 1980; Wiscombe and Warren, 1980; Aoki *et al.*, 2000; 2003). These snow parameters are uncertain factors for the recent drastic snow/ice melting in the Arctic (Aoki *et al.*, 2011). The Greenland ice sheet (GrIS), in particular, is presently undergoing drastic changes (Steffen *et al.*, 2008; van den Broeke *et al.*, 2009; Rignot *et al.*, 2011). When air temperature increases, snow grain size also increases because of accelerated snow metamorphism and albedo is thus reduced (positive albedo feedback) (Box *et al.*, 2012). This process is dominant mainly in the accumulation areas of the GrIS.

Light-absorbing snow/ice impurities include black

carbon (BC), organic carbon (OC), mineral dust and, in the broad sense, glacial microbes. BC concentration in GrIS has been measured from ice cores (Chýlek *et al.*, 1987, 1995; McConnell *et al.*, 2007) and snow samples (Clarke and Noone, 1985; Chýlek *et al.*, 1987, 1995; Hagler *et al.*, 2007; Doherty *et al.*, 2010, 2013; Carmagnola *et al.*, 2013). Most of the presently measured BC concentrations are less than several parts per billion by weight (ppbw), and such levels of BC concentration would not have a significant impact on albedo reduction when snow is not melting. However, the possible albedo reduction due to BC of in-situ measured maximum value on northwest GrIS in 2012 was estimated to be 0.03 (Aoki *et al.*, 2014), and this reduction could be enhanced further for large snow grain size under a heavy melting condition. Climate modeling studies have shown that BC in snow exhibits positive radiative forcing on Climate and is a possible cause of snow melting in the Arctic (Hansen and

Nazarenko, 2004; Flanner *et al.*, 2007, 2009).

Dust could also contribute to albedo reduction, but light absorption by dust in the visible region is lower than that of BC by 1/160 (Aoki *et al.*, 2011). On the other hand, the bare ice area is extended by snow melting on ice associated with air temperature increase in ablation areas (van den Broeke *et al.*, 2011). It was recently reported that wide bare-ice areas in GrIS are covered with mineral dust and glacial microbes whose albedos are lower than that of blue ice surface (Wientjes *et al.*, 2011, 2012). The albedo reduction by glacial microbes is also a positive albedo feedback effect as the microbes usually grow on melting Glacier surface (Takeuchi *et al.*, 2002).

Drastic snow/ice melting is occurring in the Arctic, as mentioned above, but the predictions made by general circulation models (GCMs) for the cryosphere in the Arctic are insufficient. One possible reason for this insufficiency is that most of the snow/ice albedo schemes employed in GCMs are parameterized empirically (*e.g.*, Pedersen and Winther, 2005; Brun *et al.*, 2008). It is thus necessary to develop or improve a physically based snow albedo model for use in combination with a snow metamorphism scheme. Aoki *et al.* (2011) explained that the following issues need to be addressed: (1) the optical properties of the presently used light-absorbing snow impurities (BC and dust) should be validated, (2) brown carbon or organic carbon should be introduced as an additional snow Impurity, (3) a model of glacial microbial activities on Glaciers and ice sheets should be developed, (4) the snow metamorphism model should be improved to calculate the optically equivalent snow grain size and (5) the global applicability of the models should be validated.

To elucidate the snow/ice albedo feedback effect caused by snow grain growth and light-absorbing snow/ice impurities, including glacial microbes, for the recent abrupt snow/ice melting in the Arctic, the Snow Impurity and Glacial Microbe effects on abrupt warming in the Arctic (SIGMA) Project was launched in 2011. The SIGMA Project consists of (1) field campaigns in Greenland from 2011 to 2014, (2) continuous meteorological and glaciological observations in snow-covered areas of Japan from 2011 to 2015, (3) Climate modeling using a GCM in which a snow metamorphism model (Niwan *et al.*, 2012) is incorporated, (4) satellite remote sensing for snow physical parameters and (5) ice core drilling on GrIS in 2014. In this paper, the field activities of the SIGMA Project in Greenland during 2011–2013 are reported. The candidate activity areas in Greenland at the project outset were the Qaanaaq area in northwest Greenland and the Ilulissat and Kangerlussuaq areas in mid-west Greenland. We chose these areas with consideration to accessibility and changing tendencies of snow/ice. Based on the field reconnaissance conducted in 2011, we finally chose the Qaanaaq area as our main activity area and the Kangerlussuaq area for a portion of the biological observations. For the Qaanaaq area, we placed

importance on a balance of our activities with existing observation stations and activities (sparse observation area). The Qaanaaq area as well as southwest Greenland is also an area potentially more affected by global warming compared to the east Greenland in the future (Rae *et al.*, 2012; Fettweis *et al.*, 2013). The Kangerlussuaq area, as a developing dark region the in ablation zone (Wientjes *et al.*, 2011), is important for our biological studies.

The ice cap that we studied extends to the north of the village of Qaanaaq, located in northwestern Greenland, covers an area of 289 km², and has an elevation range of 30–1,110 m a.s.l. over the central part of a peninsula. The name of the ice cap is not indicated in a map of Asiaq published by The Greenland Survey (<http://en.nunagis.gl>), but the name of the land is shown as “Piulip Nuna.” Uetake *et al.* (2010) referred to it as a small ice cap (Piulip Nuna) in northwestern Greenland (77°29' N, 69°14' W), and Sugiyama *et al.* (2014) referred to it as Qaanaaq ice cap (77°28' N, 69°14' W). In accordance with Sugiyama *et al.* (2014), we refer to it in the present study as Qaanaaq ice cap (QIC).

2. Reconnaissance in 2011

Field reconnaissance observation was conducted in July and August 2011 in the Qaanaaq, Ilulissat and Kangerlussuaq areas, shown in Fig. 1. Compared with the other two areas, the Qaanaaq area has relatively sparse

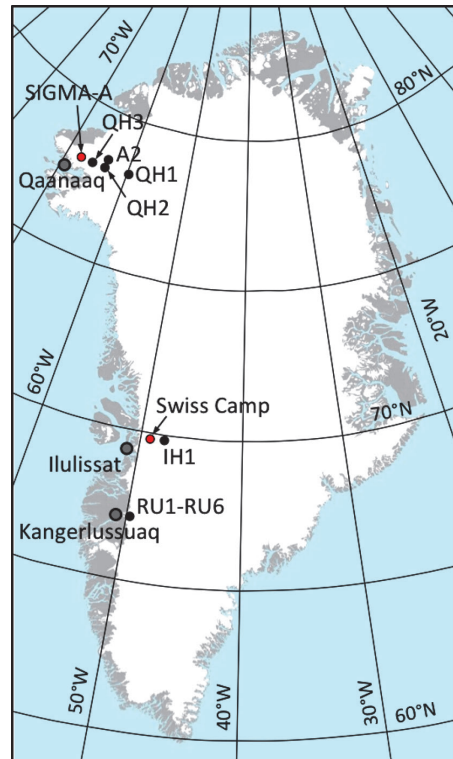


Fig. 1. Map showing the location of observation sites in the Qaanaaq (observation sites around Qaanaaq), Ilulissat (Swiss Camp and IH1) and Kangerlussuaq areas (RU1–RU6) of the SIGMA Project in Greenland. Red colored circles indicate AWS stations.

Table 1. Reconnaissance observation in 2011.

Item	Content
Overall period	July 26-August 9, 2011
Area	Qaanaaq, Ilulissat and Kangerlussuaq areas
Member	Teruo Aoki, Hideaki Motoyama, Sumito Matoba and Jun Uetake
Period	July 27-31 and August 2-3, 2011
Area	Qaanaaq ice cap (QIC) (See Figs. 2)
Observation site	QA1: $77^{\circ} 29' 27''$ N, $69^{\circ} 15' 03''$ W, $h = 247$ m a.s.l. QA2: $77^{\circ} 29' 52''$ N, $69^{\circ} 12' 43''$ W, $h = 441$ m a.s.l. QA2B: $77^{\circ} 29' 58''$ N, $65^{\circ} 10' 32''$ W, $h = 506$ m a.s.l. QA-red: $77^{\circ} 29' 56''$ N, $69^{\circ} 10' 05''$ W, $h = 565$ m a.s.l. QA3: $77^{\circ} 30' 12''$ N, $69^{\circ} 08' 45''$ W, $h = 668$ m a.s.l. QA4: $77^{\circ} 30' 27''$ N, $69^{\circ} 07' 19''$ W, $h = 778$ m a.s.l.
Member	TA, SM and JU
Access	Foot
Observation method or item	Snow pit observation, snow and ice sampling, spectral albedo measurement, glacial sediment sampling, melt water sampling and cryoconite hole observation
Date	August 1, 2011
Area	GrIS in Qaanaaq area (See Figs. 1 and 4)
Observation site	QH1: $77^{\circ} 54' 58''$ N, $59^{\circ} 59' 34''$ W, $h = 1,992$ m a.s.l. QH2: $77^{\circ} 57' 57''$ N, $63^{\circ} 59' 36''$ W, $h = 1,681$ m a.s.l. QH3: $77^{\circ} 59' 59''$ N, $65^{\circ} 59' 52''$ W, $h = 1,469$ m a.s.l.
Member	TA, SM and JU
Access	Helicopter
Observation method or item	Snow pit observation and snow sampling
Date	August 5, 2011
Area	GrIS in Ilulissat area (See Fig. 1)
Observation site	IH1: $69^{\circ} 42' 30''$ N, $48^{\circ} 27' 01''$ W, $h = 1,506$ m a.s.l. Swiss Camp: $69^{\circ} 33' 53''$ N, $49^{\circ} 19' 51''$ W, $h = 1,176$ m a.s.l. (published position)
Member	TA, HM, SM and JU
Access	Helicopter
Observation method or item	Snow pit observation, snow and ice sampling, glacial sediment sampling, melt water sampling and cryoconite hole observation
Date	August 7, 2011
Area	Russel Glacier in Kangerlussuaq area (See Fig. 1)
Observation site	RU1: $67^{\circ} 09' 19''$ N, $50^{\circ} 01' 48''$ W, $h = 510$ m a.s.l. RU2: $67^{\circ} 09' 39''$ N, $50^{\circ} 01' 10''$ W, $h = 565$ m a.s.l. RU3: $67^{\circ} 09' 56''$ N, $49^{\circ} 58' 56''$ W, $h = 635$ m a.s.l.
Member	TA, HM, SM and JU
Access	Car and foot
Observation method or item	Glacial sediment sampling, snow and ice sampling, melt water sampling and cryoconite hole observation

coverage in terms of an automatic weather station (AWS) network (Steffen and Box, 2001; van den Broeke *et al.*, 2008; van As *et al.*, 2011). Snow algal communities on Qaanaaq Glacier in the Qaanaaq area were investigated once in 2007 (Uetake *et al.*, 2010), and those on Russel Glacier in the Kangerlussuaq area were investigated recently by several researchers (*e.g.*, Stibal *et al.*, 2012; Yallop *et al.*, 2012). In order to conduct continuous meteorological observation with an AWS, campaign observations for glaciology and meteorology and shallow ice core drilling, it was necessary to examine the snow conditions at the candidate observation sites. The details of the observation periods, sites, members, access methods, and observation methods and items are listed in Table 1. This party was composed of one meteorologist, two glaciologists and one biologist.

2.1 Qaanaaq area

We stayed in Qaanaaq from July 27 to August 3, 2011 and conducted snow pit observation, spectral albedo measurement (Aoki *et al.*, 2013) and biological observation

at several sites on Qaanaaq Glacier, which flows out of QIC (Fig. 2). It took about 3 hours by foot from Qaanaaq to access site QA4 (elevation $h=778$ m a.s.l.). We hereafter in this paper express an elevation by “ h ”. The surfaces of Qaanaaq Glacier were mostly covered with glacial microbes in ice-grain layers with a radius of 5 to 10 mm and a thickness of several cm above bare ice (Fig. 3). Many cryoconite holes had formed on the Glacier surfaces around QA4.

To examine candidate sites on GrIS, where AWS installation was planned for 2012 and a shallow ice core drilling was planned for 2014, we flew to three sites, QH1 ($h=1,992$ m a.s.l.), QH2 ($h=1,681$ m a.s.l.) and QH3 ($h=1,469$ m a.s.l.), by helicopter (Bell 212, Air Greenland) on August 1, 2011 (Fig. 4). Because the helicopter could not fly a round trip between Qaanaaq and QH1 due to the limitation of fuel consumption, we refueled at QH2 from two drums of fuel transported in advance on the return trip from QH1 to QH3. At these sites, we performed snow pit observation down to depths of 80–100 cm and snow sampling for measurement of light-absorbing

snow impurities (LASI) (Aoki *et al.*, 2014) within the sojourn time of 30 min at each site. The snow condition at QH1 consisted of dry snow, and those at QH2 and QH3 were wet snow and ice layers (Fig. 5). Hence, QH1 was regarded to be suitable as a snow and ice core drilling site where it is necessary that the snow has not melted. For an AWS site in the accumulation area, we intended a location where surface melting can be observed in summer season. The snow condition at QH3 was suitable for the AWS site. However, as the surface at QA3 was a gentle southern slope, we intended to change

the candidate site to the northwest along the ridge in the next year. As a result, we determined the candidate site for AWS as the SIGMA-A location shown in Fig. 4. From the helicopter, between Qaanaaq and the three sites on GrIS, most surfaces of QIC appeared dark.

2.2 Ilulissat area

The AWS at Swiss Camp, which has the longest observational record (since 1990) on GrIS, and four other AWSs around Swiss Camp are working in the Ilulissat area (Fig. 1). It was thus difficult to find scientific signifi-

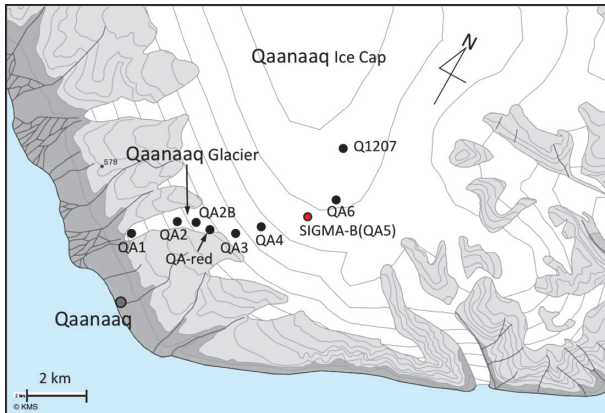


Fig. 2. Map showing the location of observation sites on the Qaanaaq Ice Cap. The contour interval is 100 m and the contour lines higher than 700 m do not agree with the site elevations measured with GPS as shown in Tables 1–3. The red colored circle is an AWS station.



Fig. 3. Cryoconite hole observation with spectral albedo measurements at QA3 ($h=668$ m a.s.l.) on Qaanaaq Glacier on July 30, 2011.

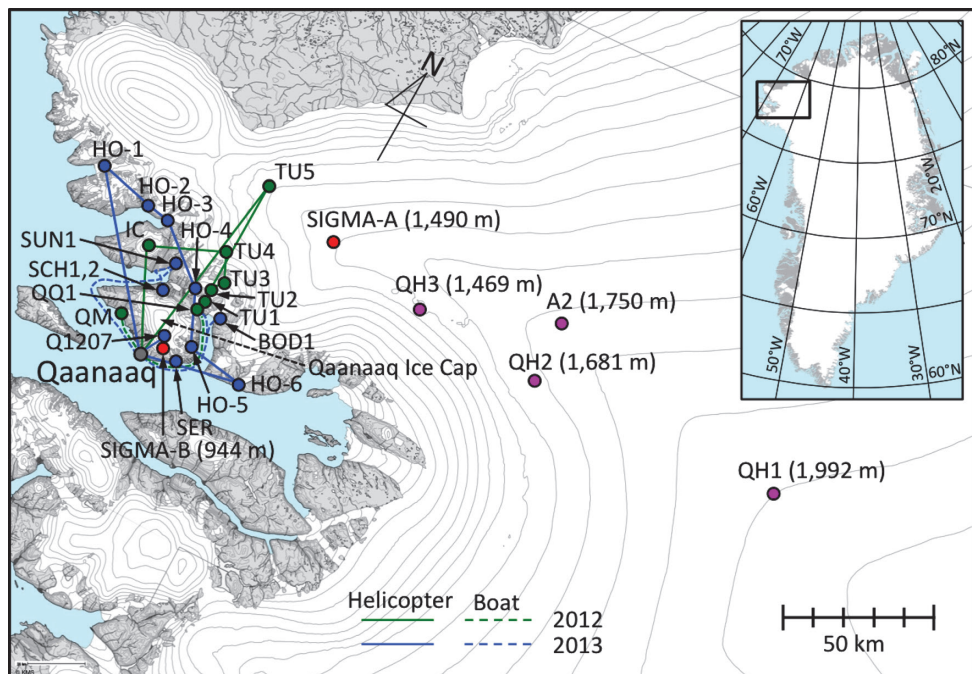


Fig. 4. Map showing the location of observation sites in the Qaanaaq area of northwest Greenland. The contour interval is 100 m. Red and pink colored circles indicate AWS stations established in 2012 and glaciological/meteorological observation sites, respectively, and the elevations are given in the parentheses. These sites were accessed by helicopter. Green and blue colored circles indicate biological observation sites in 2012 and 2013, respectively. Solid and dashed lines connected with those circles indicate the helicopter and boat routes, respectively, in each year.

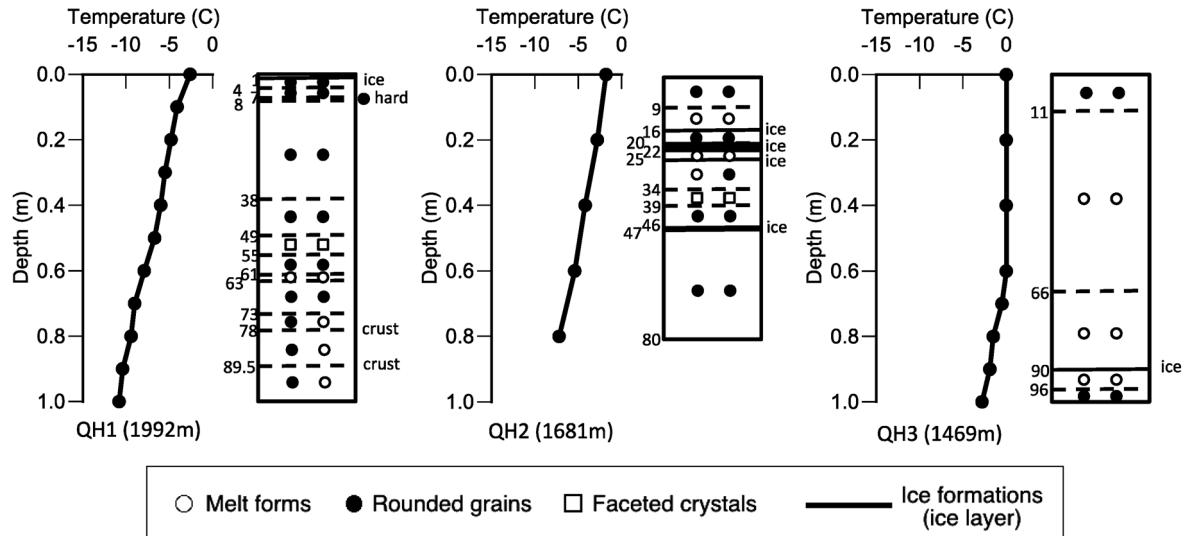


Fig. 5. Snow stratigraphy and vertical profiles of snow temperature in snow pits at sites QH1, QH2 and QH3 on July 30, 2011. The characters showing snow classification are in accordance with the snow classification by Fierz *et al.* (2009), which are indicated in the legend.

cance for adding our AWS in this area, although drastic melting is occurring here (*e.g.*, van den Broeke *et al.*, 2009; Sørensen *et al.*, 2011). We made a reconnaissance visit to a potential site for ice core drilling on August 5, 2011. As the gradient of the ice sheet surface over this region is small, a long distance flight was required from Ilulissat to reach a high elevation site. However, due to the limitation of fuel consumption of the helicopter, we flew to site IH1 ($h=1,506\text{ m a.s.l.}$) (Fig. 1 and Table 1). The snow pit down to 60 cm consisted of melt forms and ice layers. The surface looked clean, but there were some crevasses with a width of about 1 m. Therefore, the site was ineligible of our purpose.

On the return trip, we landed on the snow surface near Swiss Camp ($h=1,149\text{ m a.s.l.}$) (Steffen and Box, 2001) to collect snow/ice samples and glacial sediment samplings. The surface consisted of large snow or ice grains on bare ice, that was similar to that on Qaanaaq Glacier, and there were also some melt ponds and rivulets. The surface was covered with different types of glacial microbes, including red snow (Table 1). At this time, we confirmed that the constructions and some AWSs at Swiss Camp had collapsed due to heavy surface melting (Palmer, 2012). These were reconstructed in 2011.

2.3 Kangerlussuaq area

In the Kangerlussuaq area, the terminus area of GrIS is accessible by foot from "Point 660," which is at the end of gravel road from Kangerlussuaq and located 10 km northeast of Russel Glacier. It took one hour to travel from Kangerlussuaq to "Point 660" by 4-wheel-drive vehicle on August 7, 2011. In the marginal area up to 1.5 km from Glacier front, the Glacier surface was relatively flat and was covered with fine rock debris. Beyond this area, the Glacier surface turned to gravel due to crevasses (Fig. 6). Many cryoconite holes with



Fig. 6. Route reconnaissance for biological observation on Russel Glacier on August 7, 2011.

cryoconite at the bottom of the holes had formed in the gravel ice area. The depth of the holes appeared to be deeper than those observed in the Qaanaaq region during this season. The surface ice in this area consisted of ice grains with a size of several millimeters to several centimeters. The surface visibly appeared to be white rather than a blue or dusty color. We collected samples of surface ice and cryoconite from cryoconite holes at RU2 and RU3 (Table 1).

3. Field activities in 2012

Based on the field reconnaissance in 2011, we chose the Qaanaaq area as our main observation field, as mentioned in section 1. We here refer to the area shown in Fig. 4 as the "Qaanaaq area," which includes the northwest GrIS and ice caps and Glaciers around Qaanaaq, because similar area names will appear in the following sections. Our field activities in the 2012 summer season

Table 2. Glaciological and meteorological observations in 2012.

Item	Content
Overall period	June 11- August 1, 2012
Area	Qaanaaq area
Member ¹	Teruo Aoki, Sumito Matoba, Satoru Yamaguchi, Tetsuhide Yamasaki, Tomonori Tanikawa and Masashi Niwano
Period	Period-1 (June 11-June 25, 2012) and Period-3 (July 17-August 1, 2012)
Area	QIC and Qaanaaq (See Fig. 2)
Observation site	QA1, QA2, QA2B, QA-red, QA3 and QA4: See Table 1 SIGMA-B (= QA5): 77° 31' 06" N, 69° 03' 43" W, $h = 944$ m a.s.l. QA6: 77° 32' 25" N, 69° 04' 08" W, $h = 1,090$ m a.s.l.
Member	TA, SM, SY, TY, TT and MN
Access	Foot (helicopter for only AWS installation at SIGMA-B)
Observation method or item	AWS installation (SIGMA-B), snow pit observation, snow and ice sampling, spectral albedo measurement and all-sky camera installation at Qaanaaq Geophysical Observatory of the Danish Meteorological Institute (DMI)
Period	Period-2 (June 26-July 16, 2012)
Area	GrIS in Qaanaaq area (See Figs. 1 and 4)
Observation site	SIGMA-A: 78° 03'06" N, 67° 37'42" W, $h = 1,490$ m a.s.l.
Member	TA, SM, SY, TY, TT and MN
Access	Helicopter
Observation method or item	AWS installation, snow pit observation, snow sampling, hand-auger drilling (19 m), spectral albedo and bidirectional reflectance measurement, sunphotometer, NIR camera, snow stake measurement (16 stakes), all-sky camera and present weather

¹Two press journalists, Yumi Nakayama and Koutaro Sawano, temporally attended the field activities.

Table 3. Instruments of AWS at SIGMA-A.

Parameter	Height ¹	Instrument
Air temperature and relative humidity	3 and 6 m	Thermo-hygrometer (HMP-155, Vaisala, Finland, and Multi-plate radiation shield Model-41003, Young Co., USA)
Air pressure	2 m	Barometer (PTB210, Vaisala, Finland)
Wind speed and direction	3 and 6 m	Aerovane (Model-05130, Young Co., USA)
Snow height change	3 m	Ultrasonic snow gauge (SR50A, Campbell Scientific, Inc., USA)
Downward and upward solar radiation	1.5 m	Net radiometer (CNR-4, Kipp & Zonen, Netherlands)
Downward and upward longwave radiation	1.5 m	Net radiometer (CNR-4, Kipp & Zonen, Netherlands)
Downward and upward solar radiation in NIR spectral region	1.5 m	Pyranometer (CMP-6, Kipp & Zonen, Netherlands, and RG715 filter dome, Prede, Japan)
Snow temperature	0.4, 0.7 and 1.0 m	Thermistor thermometer (PTWP-10, Climate Inc., Japan)
Surface and sensor conditions	1.5 and 3 m	Interval camera (Garden Watch Cam, Brinno Inc., USA)
Tilt angle of AWS main pole	2 m	Inclinometer (B2N85H, Turck Inc., USA)
Data recording		Data logger (CR1000, Campbell Scientific, Inc., USA)

¹Values at the time of installation on June 29, 2012.

were (1) glaciological and meteorological observations along with the installation of two AWSs at sites SIGMA-A ($h=1,490$ m a.s.l) on GrIS and SIGMA-B ($h=944$ m a.s.l) on QIC (Table 2) in June and July, respectively, and (2) biological observations (Table 3) on QIC, GrIS and at several Glaciers around Qaanaaq in July and August. We refer to the groups of these, (1) and (2), as "SIGMA-A&B Party" and "Biology Party," respectively. The former was composed of two meteorologists, three glaciologists and one field expert, and the latter consisted of four biologists. Additionally, four glaciologists with the Green Network of Excellence (GRENE) Arctic Climate Change Research Project (MEXT, 2012) ("GRENE Party") also stayed in Qaanaaq for glaciological observa-

tions on QIC and GrIS. All parties respectively arrived at Qaanaaq several days late by regular commercial flights from Ilulissat due to adverse weather in June and July 2012. We first established a base facility called "Qaanaaq Club House" (QCH), which was a local rental house where we stayed and kept instruments and equipment, within the village of Qaanaaq in June. Because the capacity of QCH was 8–10 persons, some members stayed in local accommodations when QCH was fully occupied. The field activities by SIGMA-A&B Party are described for the three periods shown in Table 2; before flying to SIGMA-A (Period 1: June 11–June 25, 2012), at SIGMA-A (Period 2: June 26–July 16, 2012), and after returning from SIGMA-A (Period 3: July 17–August

1, 2012); in the following section. Then, field activities by Biology Party are described mainly for their activity areas and cryoconite analysis on Qaanaaq Glacier.

3.1 Glaciological and meteorological observations (SIGMA-A&B Party)

3.1.1 Qaanaaq and QIC (Period 1)

When we arrived at Qaanaaq on July 11, 2012, the fjord of Inglefield Bredning, within sight from Qaanaaq, was covered with sea ice. We stayed in Qaanaaq until August 1, 2012, except for a camping period at SIGMA-A on GrIS (Table 2). The major works at QIC were AWS installation at SIGMA-B, snow pit observation, snow and ice sampling and spectral albedo measurement. Although the original schedule for our stay at SIGMA-A was from June 19 to July 16, 2012 (28 days), the helicopter flight was postponed to June 26, 2012, due to adverse weather conditions including rainfall. Before the flight to SIGMA-A, we visited QIC for reconnaissance for the candidate site of SIGMA-B on June 24, 2012. The QIC surfaces around QA3 and QA4 were bare ice covered with cryoconite containing glacial microbes, which was similar to the condition of previous year, but the cryoconite abundance appeared to be lower than that at the end of July 2011. The upper areas at elevations higher than 800 m a.s.l on QIC were covered with snow.

3.1.2 SIGMA-A (Period 2)

A helicopter operation to SIGMA-A was made on June 26, 2012. When the helicopter approached SIGMA-A, the sky was covered with low clouds. Hence, the pilot returned and landed on another snow surface on GrIS at an elevation of about 1,250 m a.s.l. (SIGMA-A') under scattered clouds. To transport all of our equipment, instruments and six passengers, weighing a total of about 3,000 kg, three trips were necessary. During the first two trips between SIGMA-A' and Qaanaaq, we examined the snow condition at that site. The snow surface looked uniform but had a gentle southerly slope with a steeper angle toward the south. Probing the inner snowpack with a sounding rod, we found a hidden crevasse with a width of about 20 cm at a depth of about 80 cm, where there was a thick ice layer. When the pilot arrived at SIGMA-A by the third flight, we discussed additional transportation between SIGMA-A' and SIGMA-A. Fortunately, the sky condition had become clear, and we could finally move to SIGMA-A with all of our equipment and instruments (Fig. 7).

We set up a camp at SIGMA-A and stayed for three weeks from June 26, 2012. The glaciological and meteorological observations that we conducted were AWS installation, snow pit observation, snow sampling for chemical and LASI measurements (Aoki *et al.*, 2014), a 19-m firn-ice core drilling with a hand auger, spectral radiation measurements, snow grain size with a near-infrared (NIR) camera, snow stake measurement, sky condition (mainly cloud amount) with an all-sky camera, atmospheric aero-

sol measurement with a sunphotometer and visual observation of weather conditions, as shown in Table 2. For validation of our satellite-derived snow products (Aoki *et al.*, 2007; Hori *et al.*, 2007; Stamnes *et al.*, 2007) as well as routine observations under clear sky, we measured snow grain size using a hand-held lens and NIR camera and spectral albedo and bidirectional reflectance with a spectrometer under clear sky synchronized with Terra and Aqua MODIS satellite overpasses.

Fig. 8 is a photograph of the AWS installed at SIGMA-A, which measures the meteorological and snow parameters shown in Table 3. The special features of this AWS are (1) two-level measurements of air temperature, relative humidity, wind speed and direction; (2) net solar radiation measurements in the shortwave and the NIR spectral regions; (3) monitoring of the frost condition on the radiation sensors and the snow surface condition with two interval cameras; and (4) tilt angle monitoring of the main AWS pole with an inclinometer. A net radiometer sensor and NIR pyranometers were respectively set on other mounts separated from the main AWS pole, which are not shown in Fig. 8. For all instruments,



Fig. 7. Helicopter transportation to SIGMA-A ($h=1,490$ m a.s.l.) on June 26, 2012.



Fig. 8. AWS installed at SIGMA-A on June 29, 2012.

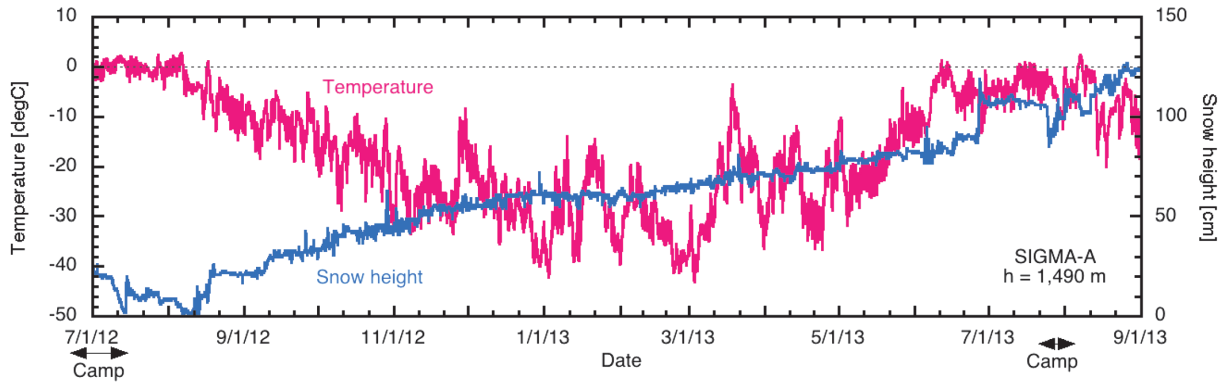


Fig. 9. Time series variation of air temperature at a height of 3m and snow height measured with an AWS at SIGMA-A from July 2012 to August 2013. Snow height is a relative value to the minimum in the summer of 2011.



Fig. 10. Drilling a 19-m firn-ice core using a hand auger at SIGMA-A on July 3, 2012.

one-minute sampling and ten-minute averaged data are stored on a data logger, and the hourly data are transported to us via Argos satellite. The electric power is supplied from cyclone batteries in the snow, which are charged by solar panels (Fig. 8).

Fig. 9 depicts variations of air temperature and snow height measured at SIGMA-A from July 2012 to August 2013. The meteorological conditions for the first half (June 24–July 9, 2012) of the observation period during which we stayed at SIGMA-A were warm (average air temperature=−0.2 °C) with a snow surface lowering of 10 cm. Subsequently, a large amount of rainfall was observed from July 10 to July 13, 2012 (average air temperature=1.3 °C), and the snow surface level decreased by 12 cm. The total precipitation amount was estimated to be in the range of 60 to 100 mm (Aoki *et al.*, 2014). During the same period, a record melting event of surface snow/ice was observed over GrIS (Nghiem *et al.*, 2012; Tedesco *et al.*, 2013). As this remarkable surface melting and the rainfall at SIGMA-A destabilized the main AWS pole and iron wire stays, we had to rebuild them.

We also conducted drilling of 19-m firn-ice cores using a hand auger on July 3 and 6, 2012 (Fig. 10) for

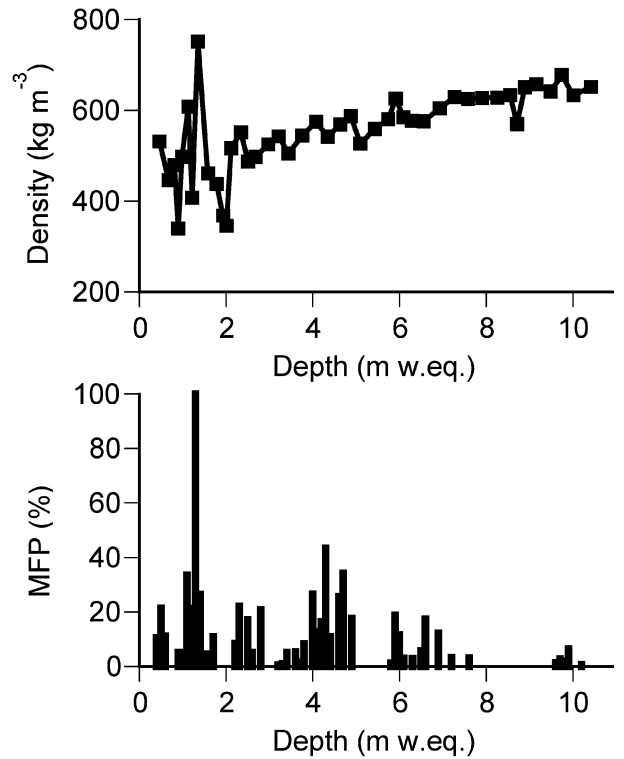


Fig. 11. Profiles of the bulk density (top) and melt feature percentage (MFP) (bottom) in a 0.1m long section (middle) of the firn-ice core obtained from SIGMA-A on July 3 and 6, 2012.

chemical analysis to reconstruct temporal variations of mass balance and depositions of chemical species at the site. The hand auger was designed by the technical division of the Institute of Low Temperature Science, Hokkaido University (ILTS-HU). We operated 36 drilling runs and obtained 19.07 m firn-ice cores, starting below the ice layer, at 0.9 m depth, that formed in the previous summer. After drilling, we observed the stratigraphy of the firn-ice cores and measured the density of each core section with an electric balance. The cores were cut horizontally into approximately 0.1-m long sections and the surface of the sections was shaved off with a stainless knife to remove any contamination attached to the surface of the firn-ice core samples during drilling and han-

dling. The decontaminated samples were packed into clean polyethylene bags, melted at ambient temperature and decanted into clean polypropylene bottles. The bottles were transported to ILTS-HU and sealed until chemical analysis was performed. Fig. 11 depicts the profiles of the bulk density and melt feature percentage (MFP) of the firn-ice core. Bulk density ranges from 480 to 670 kg m⁻³ except for the high variation layers above a depth of 2.1 m water-equivalent (w. eq.). High MFP values appear frequently in the upper layers above a depth of 7 m w. eq. and are almost zero for the older period below a depth of 8 m w. eq. suggesting that more frequent snow melting events have occurred in recent years.

On July 16, 2012, we returned to Qaanaaq using three helicopter trips. At that time, most surfaces of QIC, except the summit, appeared dark, which indicated that most of the snow cover on the ice cap had melted and that the surfaces were covered with glacial microbes.

3.1.3 Qaanaaq and QIC (Period-3)

After returning to Qaanaaq, we examined the candidate AWS site around $h=1,000$ m a.s.l. on QIC where the surface was flat. However, there were some crevasses with a width of 1–2 m along the contour line in the area at $h>960$ m a.s.l. Therefore, we installed an AWS at the position of SIGMA-B at $h=944$ m a.s.l. (Fig. 2 and Table 2) where there is a southern slope with an angle of approximately 5°. The installation was conducted on July 19, 2012 by transporting the instruments using a helicopter. Fig. 12 is a photograph of the AWS which measures the meteorological and snow parameters shown in Table 4. The figure shows that the surface was slushy and covered with snow or ice grains containing dark material. This site was used as the biological observation site, QA5, as well. The AWS measures meteorological parameters at one level as well as shortwave and longwave radiation components. It is also equipped with an interval camera and inclinometer. The data logger and power supply system were the same as that of the AWS at SIGMA-A. After installing the AWS, a remarkable surface lowering of 53 cm, until August 10, 2012, was observed during 22

days of positive air temperatures as shown in Fig. 13, which depicts the variation of air temperature and snow height measured at SIGMA-B from July 2012 to August 2013. Sugiyama *et al.* (2014) reported that the dark surface contributed to a heavy melting of the ice surface of QIC in the summer of 2012.

The main activities other than AWS installation on QIC were snow pit observation, spectral albedo measurement and snow and ice sampling. Spectral albedos were measured together with snow and ice sampling to investigate the effect of glacial microbes at the sites of QA2B, QA-red, QA3 and QA5 (Fig. 2) on July 18 and 20, 2012. We also installed an all-sky camera, which was the same instrument as that used at SIGMA-A, at the Qaanaaq Geophysical Observatory of the Danish Meteorological Institute (DMI) to monitor the sky condition throughout the year.

3.2 Biological observations (Biology Party)

3.2.1 QIC area

During the period from July 18 to August 3, 2012, we collected ice samples of the Glacier surface and measured the spectral reflectivity of the surface and dimensions of cryoconite holes at sites QA1-QA6, QA-red, QM, QQ1



Fig. 12. AWS installed at SIGMA-B ($h=944$ m a.s.l.) on July 19, 2012.

Table 4. Instruments of AWS at SIGMA-B.

Parameter	Height ¹	Instrument
Air temperature and relative humidity	3 m	Thermo-hygrometer (HMP-155, Vaisala, Finland, and Multi-plate radiation shield Model-41003, Young Co., USA)
Air pressure	1 m	Barometer (PTB210, Vaisala, Finland)
Wind speed and direction	3 m	Aerovane (Model-05130, Young Co., USA)
Snow height change	3 m	Ultrasonic snow gauge (SR50A, Campbell Scientific, Inc., USA)
Downward and upward solar radiation	2.5 m	Net radiometer (CNR-4, Kipp & Zonen, Netherlands)
Downward and upward longwave radiation	2.5 m	Net radiometer (CNR-4, Kipp & Zonen, Netherlands)
Surface condition	1.5 and 3 m	Interval camera (Garden Watch Cam, Brinno Inc., USA)
Tilt angle of AWS main pole	2 m	Inclinometer (B2N85H, Turck Inc., USA)
Data recording		Data logger (CR1000, Campbell Scientific, Inc., USA)

¹ Values at the time of installation on July 19, 2012.

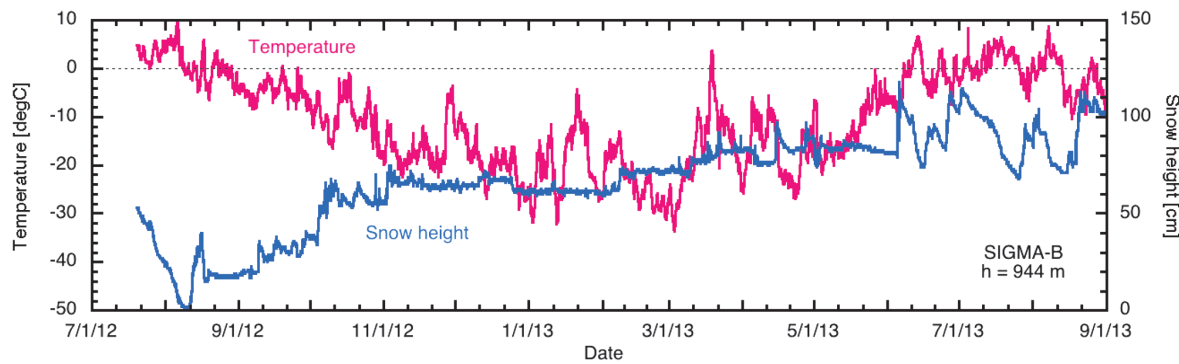


Fig. 13. Time series variation in air temperature at a height of 3m and snow height measured with AWS at SIGMA-B from July 2012 to August 2013. Snow height is a relative value to the minimum in the summer of 2011.

Table 5. Biological observations in 2012.

Overall period	July 16-August 8, 2012
Area	Qaanaaq and Kangerlussuaq areas
Member ¹	Nozomu Takeuchi, Jun Uetake, Naoko Nagatsuka and Rigen Shimada
Period	July 16-August 3, 2012
Area	QIC (See Fig. 2)
Observation site	QA1, QA2, QA2B, QA-red, QA3 and QA4: See Table 1 QA5 (= SIGMA-B) and QA 6: See Table 2 QA6: See Table 2
Member	NT, JU, NN and RS
Access	Foot
Observation method or item	Meteorological observation, ice surface conditions, albedo measurement, glacial microbe sampling, glacial sediment sampling, snow and ice sampling, melt water sampling, cryoconite hole observation and interval camera
Date and member	July 27-28, 2012 (NT, JU, NN and RS) August 2, 2012 (JU and RS)
Area	Glaciers around QIC (See Fig. 2)
Observation site	QQ1 (Qaqortaaq Glacier): 77° 40' 06" N, 68° 49' 11" W, $h = 42$ m a.s.l. TU1 (Tugto Glacier): 77° 40' 50" N, 68° 51' 12" W, $h = 54$ m a.s.l. QM (northwestern glacier near Fan Glacier): 77° 36' 07" N, 69° 42' 16" W, $h = 605$ m a.s.l.
Access	Boat
Observation method or item	Ice surface conditions, albedo measurement, glacial microbe sampling, glacial sediment sampling, snow and ice sampling, melt water sampling and cryoconite hole observation
Date	July 30, 2012
Area	GrIS and ice cap around QIC (See Fig. 4)
Observation site	TU2: 77° 45' 20" N, 68° 45' 52" W, $h = 333$ m a.s.l. TU3: 77° 48' 53" N, 68° 35' 46" W, $h = 500$ m a.s.l. TU4: 77° 53' 41" N, 68° 46' 25" W, $h = 1,001$ m a.s.l. TU5: 78° 07' 00" N, 68° 54' 40" W, $h = 1,259$ m a.s.l. IC: 77° 45' 21" N, 69° 57' 38" W, $h = 973$ m a.s.l.
Member	NT, JU, NN and RS with GRENE members (Shin Sugiyama, Daiki Sakakibara and Satoshi Matsuno)
Access	Helicopter
Observation method or item	Ice surface conditions, albedo measurement, glacial microbe sampling, glacial sediment sampling, snow and ice sampling, melt water sampling and cryoconite hole observation
Date and member	August 3-5, 2012 (NT and NN) August 10, 2012 (JU and RS)
Area	Russel Glacier in Kangerlussuaq area (See Fig. 1)
Observation site	RU1: 67° 09' 19" N, 50° 01' 48" W, $h = 508$ m a.s.l. RU4: 67° 10' 50" N, 49° 48' 38" W, $h = 761$ m a.s.l. RU5: 67° 08' 52" N, 49° 44' 15" W, $h = 838$ m a.s.l.
Access	Car and foot
Observation method or item	Ice surface conditions, albedo measurement, glacial microbe sampling, glacial sediment sampling, snow and ice sampling, melt water sampling and cryoconite hole observation

¹Two press journalists, Yumi Nakayama and Koutaro Sawano, temporarily attended the field activities.

and TU1 on QIC (Fig. 2, Fig. 4 and Table 5). The Glacier surface condition of the sampling sites was ice except at the highest site of Qaanaaq Glacier (QA6) during the observation period. The Glacier surface at QA6 was snow throughout this summer season. The collected samples were transported to Japan and were analyzed for carbon weight, water dissolved ion, isotopes of minerals and counting of microorganisms and deoxyribonucleic acid (DNA) sequences. On July 18, 2012, we installed a simple AWS, consisting of an interval digital camera, thermistor thermometers at different heights and in the ice and pyranometers for downward and upward solar radiations, at QA3 (Table. 6). The data collection interval was one hour. To observe the temporal change in the cryoconite holes, another interval camera (Garden Watch, Brinno Inc., Taiwan) was installed near the AWS.

After the investigation on the Qaanaaq Glacier, we visited Qaqortaq Glacier and Tugto Glacier located on the opposite side of the Qaanaaq Glacier using a local hunter's boat. Qaqortaq Glacier is an outlet Glacier of QIC and flows toward the east (Table 5). Tugto Glacier is an outlet Glacier from GrIS, and the Glacier front is located just next to the Qaqortaq Glacier. Both Glaciers face each other across the end moraine, which originated from both Glaciers. The ablation surface of Qaqortaq Glacier was covered with a mahogany colored mineral particle, and running meltwater on the Glacier appeared to be of the same color. In contrast, mineral particles covered on TU1 were gray and clearly different from those on QQ1. We collected surface ice samples and measured the spectral reflectivity at the sites of QQ1 and TU1 on July 27 and 28, 2012.

On August 2, 2012, we tried to access Fan Glacier, which is the largest outlet Glacier from the QIC. As the proglacial river of the Glacier was deep and fast, we could not cross over and reach this Glacier. Instead, we visited a small nameless Glacier located north of Fan Glacier, following the Four Mile Dal dog sledge route. The shape of the Glacier viewed in a satellite image is similar to the cephalic lobe of a manta ray, and so, we refer to a site on this Glacier as QM (Qaanaaq's Manta). We collected ice samples and measured the spectral reflectivity in the same manner as mentioned previously.

3.2.2 Abundance of large cryoconite granules on Qaanaaq Glacier

Samples of Glacier surface ice were taken at six sites on Qaanaaq Glacier (QA1-QA5 and QA-red). At each site, five samples were collected from a randomly selected surface with an area of approximately 30×30 cm. The samples were kept frozen at -40°C in a deep freezer and transported to the National Institute of Polar Research, Japan. Ice samples including cryoconite were filtered through six different mesh size filters ranging from $1000\text{ }\mu\text{m}$ to $30\text{ }\mu\text{m}$, because size classification may allow to compare frequency of sediments granulation by microorganisms between each different sampling sites. At first, samples were filtered through a $1000\text{ }\mu\text{m}$ meshed filter with washing with ultra-pure water, and then the filtrate was filtered again through a smaller mesh size ($750\text{ }\mu\text{m}$). The same procedure was continued until the filtration cut off of $30\text{ }\mu\text{m}$. Samples of each cut off were dried for one night at a constant temperature oven at 60°C and the carbon weight of samples were measured by a nitrogen and carbon (CN) analyzer (SUMIGRAPH NC-220F: Sumika Chemical Analysis Service, Japan). We classified the cryoconite as large (diameter more than $250\text{ }\mu\text{m}$) and small (diameter from 30 to $250\text{ }\mu\text{m}$) according to the morphology of each grain under a microscope.

Fig. 14 shows the amounts of carbon (g m^{-2}) of large cryoconite granules (diameter more than $250\text{ }\mu\text{m}$) from sites QA1-QA5 and QA-red. On Qaanaaq Glacier, the carbon amounts at QA3 and QA4 were higher than those at the other sites (QA1, QA2 and QA-red). This result indicates that cryoconite granules developed well specially at QA3 and QA4. Although a cryoconite granule is known as the aggregation of microorganisms (mainly formed by filamentous cyanobacteria) and mineral particles (*e.g.* Takeuchi *et al.*, 2005), the amount of large cryoconite granules may correspond to cell concentrations of filamentous cyanobacteria. We did not measure the cell concentration of microorganisms in these samples, but previous studies have shown that filamentous cyanobacteria dominate at same sites (Uetake *et al.*, 2010). On Qaanaaq Glacier, the partial distribution of large cryoconite granules could be caused by some environmental factors to support the growth of filamentous cyanobacteria; however, these factors are uncertain. Measurements

Table 6. Instruments of a simple AWS and interval camera at QA3.

Parameter	Height ¹	Instrument
Air temperature	0.1, 0.5, 1.0, 1.5 and 2.0 m	Thermistor thermometer (Pt100, Hakusan, Japan)
Ice surface temperature	Ice surface	Thermistor thermometer (Pt100, Hakusan, Japan)
Downward and upward solar radiation	1.5 m	Pyranometer (MS402, Eko, Japan)
Surface condition	0.5 m	Interval camera (KADEC21-EYEII: North One, Japan and Garden Watch Cam, Brinno Inc., Taiwan)
Data recording		Data logger (DATAMARK LS-3000PtV: Hakusan, Japan)

¹ Values at the time of installation on July 18, 2012.

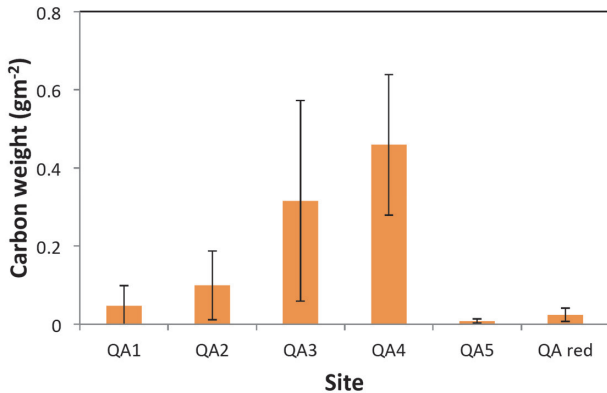


Fig. 14. Amounts of carbon weight (g m^{-2}) of large cryoconite (more than 250 mm in diameter) from QA1 to QA5 and QA-red.

of the optimum growth condition (*e.g.* photosynthesis active radiation, temperature and nutrient concentrations) of filamentous cyanobacteria by incubation of experiments may be necessary to identify the factors.

3.2.3 Upward of Tugto Glacier (GrIS)

A helicopter operation to GrIS was made on June 30, 2012. First, we planned to access the north slope of GrIS near the Inglefield Land, which is the unglaciated land located 90 km north of Qaanaaq. However, we could not approach it due to cloud cover in the area. Instead, we landed at four sites along the Tugto Glacier (TU2-TU5), which flows southward from GrIS, and one site on a small ice cap located in the north of the QIC (IC). The surface condition at TU4, TU5 and IC was snow and that at TU2 and TU3 was ice. At all the sites, we collected surface snow/ice samples for carbon weight, water dissolved ion, isotopes of minerals, microbe cell counting and DNA analysis, and also measured the spectral reflectivity of the surface.

3.2.4 Kangerlussuaq area

During August 3–5, 2012, surface ice collections and measurement of cryoconite hole dimensions were conducted at RU1, RU4 and RU5 (Table. 5). Access to the terminus of GrIS was the same as in 2011. RU4 and RU5 were located further inland as compared to the sites of 2011, and RU5 is located in the border of the clean ice area and dark region that was referred to by Wientjes *et al.* (2012). The sites were accessed by foot along a large supraglacial stream and it took approximately 6 hours to RU4 and another 4 hours to RU5.

4. Field activities in 2013

Field investigations by the SIGMA Project in 2013 were conducted by two groups, SIGMA-A&B and the Biology Party. The Biology Party arrived at Qaanaaq earlier than the SIGMA-A&B Party, at the end of June 2013, for long-term monitoring of glacial microbes on QIC

and their effects on albedo. However, most surfaces of QIC were covered with snow at that time. The GRENE Party also arrived at Qaanaaq at the same time for glaciological observations in Bowdoin Glacier and QIC. The Biology and SIGMA-A&B Party comprised of four and six persons, respectively, and the GRENE Party consisted of five persons together with three television crews. The field activities of the SIGMA-A&B Party, which were done in three periods shown in Table 7, as is the case in section 3.1 for 2012, are described in section 4.1, and those of the Biology Party in their activity areas are described in section 4.2.

4.1 Glaciological and meteorological observations (SIGMA-A&B Party)

4.1.1 Qaanaaq and QIC (Period-1)

Field observations by the SIGMA-A&B Party in 2013 were basically the same as those in 2012, except for the AWS maintenance (Table 7). We arrived at Qaanaaq on July 18, 2013 and stayed in Qaanaaq and SIGMA-A for three weeks. We visited AWS at SIGMA-B for maintenance on July 20, 2013 and retrieved the ten-minute interval data stored in the data logger, which is not transmitted via the Argos satellite in real time. The surface conditions at QIC at that time were quite different from those during the same period in 2012. Surfaces in large areas with elevations higher than about 700 m were covered with snow. The increase in snow height measured by the AWS at SIGMA-B on that day from the minimum value of 2012 that was recorded on August 10, 2012, was +78 cm (Fig. 13), and this consisted of 60 cm of snow and 18 cm of superimposed ice. The final change in snow surface height from September 1, 2012 to the same day in 2013 was +83 cm.

4.1.2 SIGMA-A (Period-2)

We flew to SIGMA-A on July 23, 2013 and stayed there for one week. The surface snow condition when we arrived at SIGMA-A was dry and quite different from that in the middle of July 2012 (highly wet). The snow height had increased by approximately 100 cm from the minimum value in 2012 that was recorded on August 8, 2012. We lifted the AWS and radiation instruments by inserting 120 cm long extension poles. This gap in the snow height record is corrected in Fig. 9, which shows a small dip around July 24, 2013 that was due to maintenance, but it was buried with snowfall and drifting snow after that. The final annual change in snow surface height from September 1, 2012 to the same day in 2013 was +117 cm. The monthly averaged air temperature in July was -4.1°C , which is 3.9°C colder than that in 2012. As there was heavy blowing snow during the period from July 25 to July 28, 2013, some cables connecting the radiation sensors and data logger, which were packed in an ice layer, could not be dug from the snowpack although the data logger and battery box were able to be dug up. We were also able to retrieve the

Table 7. Glaciological and meteorological observations in 2013.

Item	Content
Overall period	July 18-August 7, 2013
Area	Qaanaaq area
Member	Teruo Aoki, Sumito Matoba, Tetsuhide Yamasaki, Tomonori Tanikawa, Masashi Niwano and Akane Tushima
Period	July 18-22, 2013 (Pariod-1) and July 31-August 7, 2013 (Pariod-3)
Area	QIC and Qaanaaq (See Fig. 2)
Observation site	QA1, QA2, QA2B, QA-red and QA3: See Table 1 SIGMA-B (=QA5): See Table 2
Member	TA, SM, TY, TT, MN and AT
Access	Foot
Observation method or item	AWS maintenance (SIGMA-B), snow pit observation, snow and ice sampling spectral albedo measurement and all-sky camera maintenance (Qaanaaq Geophysical Observatory of DMI)
Period	July 23-30, 2013 (Pariod-2)
Area	GrIS in Qaanaaq area (See Figs. 1 and 4)
Observation site	SIGMA-A: See Table 2
Member	TA, SM, TY, TT, MN and AT
Access	Helicopter
Observation method or item	AWS maintenance, snow pit observation, snow sampling, hand-auger drilling (5 m in depth), spectral albedo measurement, NIR camera, snow stake measurement (16 stakes) and present weather
Date	July 30, 2013
Area	GrIS in Qaanaaq area (See Figs. 1 and 4)
Observation site	SIGMA-A2: $78^{\circ} 06' 13''$ N, $64^{\circ} 04' 59''$ W, $h = 1,750$ m a.s.l.
Member	SM, TY and AT with GRENE members (Shin Sugiyama, Takanobu Sawagaki, Shun Tsutaki and Mihiro Maruyama)
Access	Helicopter
Observation method or item	Snow pit observation, snow sampling and hand-auger drilling (5 m)

ten-minute interval data of the AWS successfully. Due to this severe weather condition, some meteorological and glaciological observations were canceled.

A snow pit observation was conducted on July 29, 2013 from the surface to 132 cm deep. The underlying layer was melt-freeze crust, which is likely to have been the melting snow surface in the previous summer. The major snow shapes above 132 cm were dry snow crystals including some thin ice layers, which were precipitation particles from the surface to 20 cm deep, decomposing and fragmented precipitation particles and faceted crystals from 33 cm to 91 cm deep, and depth hoar below 78 cm. This result indicates that remarkable snow melting did not occur over the last year at SIGMA-A.

The observations that were finally conducted are listed in Table 7 in which snow pit observation, snow sampling, firn-ice core drilling with a hand auger, spectral albedo measurement and NIR camera measurements were performed only on July 29, 2013. A firn-ice core drilling using a hand auger was also limited to a depth of 5 m. However, snow samplings for LASI and snow stake measurements were conducted for the entire period that we stayed at SIGMA-A. The snow height increased by about 10 cm due to snowfall during the period. On July 30, 2013, we returned to Qaanaaq by two helicopter trips. In the helicopter from SIGMA-A to Qaanaaq, we confirmed that almost all surfaces of QIC were covered with snow, which is quite different from the situation in the summer of 2012.

4.1.3 Qaanaaq and QIC (Period-3)

After returning by flight from SIGMA-A to Qaanaaq Airport, we flew to SIGMA-A2 ($h=1,750$ m a.s.l.) by helicopter on July 30, 2013 (Table 7), where we performed a snow pit observation down to 1.45 m deep. We observed the stratigraphy of the snowpack, measured the density of snow layers and collected snow samples for chemical analysis. We also obtained a 6.69 m-long firn-ice core with a hand auger, starting at below 0.64 m from the snow surface. We observed the stratigraphy of the firn-ice cores, measured the density of each ice core, and carried out decontamination and sampling from the ice cores for chemical analysis. Snow and ice core samples were transported to QCH and melted and bottled into polypropylene bottles. The bottles were transported to ILTS-HU and sealed until chemical analysis. This observation was performed in collaboration with the GRENE Party.

We conducted AWS maintenance at SIGMA-B and spectral albedo measurements with snow/ice sampling at sites QA5 (=SIGMA-B), QA3, QA-red and QA2B (Fig. 2) on August 3 and 4, 2013. In Qaanaaq, we moved the all-sky camera from the main building of the Qaanaaq Geophysical Observatory of DMI to the ionosphere observation hut located in the westward suburbs of Qaanaaq village to avoid light pollution within the village.

4.2 Biological observations (Biology Party)

4.2.1 QIC area

During the period from June 28 to August 4, 2013,

Table 8. Biological observations in 2013.

Item	Content
Overall period	June 27-August 7, 2013
Area	Qaanaaq area and Kangerlussuaq area
Member	Nozomu Takeuchi, Jun Uetake, Naoko Nagatsuka and Yukihiko Ohnuma
Period	July 18-22 and July 31-August 7, 2013
Area	QIC and Qaanaaq (See Fig. 2)
Observation site	QA1, QA2, QA2B, QA-red, QA3 and QA4: See Table 1 QA5 (= SIGMA-B) and QA 6: See Table 2
Member	NT, JU, NN and YO
Access	Foot
Observation method or item	Meteorological observation, ice surface conditions, albedo measurement, glacial microbe sampling, glacial sediment sampling, snow and ice sampling, melt water sampling, incubation on the glacier, cryoconite hole observation and interval camera
Date	July 20-21, July 24 and 26, 2013
Area	Glaciers around QIC (See Fig. 4)
Observation site	SUN1 (Sun Glacier): $77^{\circ} 46' 36''$ N, $69^{\circ} 27' 18''$ W, $h = 102$ m. SCH1 (Scarlet Heart Glacier): $77^{\circ} 39' 56''$ N, $69^{\circ} 27' 03''$ W, $h = 140$ m a.s.l. SCH2 (Scarlet Heart Glacier): $77^{\circ} 39' 13''$ N, $69^{\circ} 25' 36''$ W, $h = 324$ m a.s.l. QQ1: $77^{\circ} 40' 06''$ N, $68^{\circ} 49' 11''$ W, $h = 42$ m a.s.l. SER1 (Sermiarssupaluk): $77^{\circ} 30' 05''$ N, $68^{\circ} 45' 24''$ W, h : unknown BOD1 (Bowdoin Glacier): $77^{\circ} 40' 09''$ N, $68^{\circ} 34' 58''$ W, $h = 48$ m a.s.l.
Member	NT, JU, NN and YO with GRENE members (Shin Sugiyama, TS, Shun Tsutaki and MM)
Access	Boat
Observation method or item	Ice surface conditions, albedo measurement, glacial microbe sampling, glacial sediment sampling, snow and ice sampling, melt water sampling and cryoconite hole observation
Period	July 30, 2013
Area	QIC (See Figs. 2 and 4)
Observation site	Q1207: $77^{\circ} 32' 25''$ N, $69^{\circ} 04' 07''$ W, $h = 1,079$ m a.s.l.
Member	NT and NN with GRENE members (Takanobu Sawagaki, Daiki Sakakibara and Mihiro Maruyama)
Access	Helicopter
Observation method or item	Snow pit observation and snow sampling
Period	August 2-3, 2013
Area	Russel Glacier in Kangerlussuaq area (See Fig. 1)
Observation site	RU6: $67^{\circ} 10' 06''$ N, $50^{\circ} 02' 48''$ W, $h = 555$ m a.s.l.
Member	NT and NN
Access	Bicycle and foot
Observation method or item	Ice surface conditions, glacial microbe sampling, glacial sediment sampling, snow and ice sampling, melt water sampling and cryoconite hole observation
Date	August 6, 2013
Area	Outflow glaciers from GrIS in Qaanaaq area (See Fig. 4)
Observation site	HO-1 (Morris Jesup Glacier): $77^{\circ} 53' 16''$ N, $71^{\circ} 08' 21''$ W, h : unknown HO-2 (Meehan Glacier): $77^{\circ} 52' 28''$ N, $70^{\circ} 18' 46''$ W, h : unknown HO-3 (Verhoeff Glacier): $77^{\circ} 51' 38''$ N, $69^{\circ} 52' 08''$ W, h : unknown HO-4 (Glacier next of Tugto Glacier): $77^{\circ} 43' 29''$ N, $69^{\circ} 02' 48''$ W, h : unknown HO-5 (Syd Glacier): $77^{\circ} 33' 37.2''$ N, $68^{\circ} 42' 17.9''$ W, h : unknown HO-6 (Hubbard Glacier): $77^{\circ} 32' 17''$ N, $67^{\circ} 49' 19''$ W, h : unknown
Member	JU, AT, YO with GRENE member (ST)
Access	Helicopter
Observation method or item	Ice surface conditions, glacial microbe sampling, glacial sediment sampling, snow and ice sampling, melt water sampling and cryoconite hole observation

we collected surface ice samples and measured the spectral reflectivity on the surface and cryoconite hole dimensions at sites QA1-QA6, QA-red, SUN1, SCH1, SER1, BOD1 and QQ1, respectively (Table 8). The surface condition on the Qaanaaq Glacier in 2013 was considerably different from that in 2012. The surface was ice at QA1 and QA2 and snow at QA3, QA4, QA5 and QA6 on the Qaanaaq Glacier even though the surface condition at all these sites was ice in 2012. The collected samples were transported to Japan and will be analyzed for the

same factors as in 2012, including carbon weight, water dissolved ion, isotopes of mineral, counting of microorganisms and DNA sequences. For this reason, we took samples from Qaanaaq Glacier only one time at the end of July. In addition, we performed albedo measurement, snow pit observation and sample collection at site QA-red once every 1 or 2 weeks to observe the temporal change of the surface microbial community and its effect on the surface albedo. The physical parameters of snow recorded in the snow pit observation were snow type, snow

Table 9. Instruments of a simple AWS at QA2.

Parameter	Height ¹	Instrument
Air temperature	0.5 and 1.0 m	Thermo recorder (TR-71U, T&D, Japan)
Downward and upward solar radiation	1.5 m	Pyranometer (ML-020, Eko, Japan)
Data recording for radiation components		Data logger (LR5041: Hioki, Japan)

¹Values at the time of installation on July 9, 2013.

grain size, density, temperature and water content. On July 9, 2013, we installed a simple AWS near QA2 to measure the air temperature and solar radiation (Table 9).

After the sea ice disappeared from the fjord in front of Qaanaaq, we accessed the Glaciers around the Qaanaaq area by boat. On July 20 and 21, 2013, we visited Sun Glacier and Scarlet Heart Glacier using a local hunter's boat. Sun Glacier is an outlet Glacier from GrIS, and has a curving front at sea. Scarlet Heart Glacier flows from QIC toward the north (Table 8). The surface of Scarlet Heart Glacier was covered by mahogany colored mineral particles, which is similar to that observed on Qaqortaq Glacier, and the Glacier runoff also appeared to be the same color. On July 24 and 26, 2013, we visited the Qaqortaq, Sermiarssupaluk and Bowdoin Glaciers by boat. Sermiarssupaluk flows from QIC toward the east and Bowdoin Glacier is an outlet Glacier from GrIS that was glaciologically investigated by the GRENE Party. On these Glaciers we collected surface ice samples (Fig. 15), but measured the spectral reflectivity and cryoconite hole dimension at only BD1.

4.2.2 Outlet Glaciers from GrIS and QIC

We had planned to again access the north slope of GrIS in the Inglefield Land by helicopter, but could not due to bad weather. On August 6, 2013, the weather in the morning was rain with relatively good visibility only in the low altitude areas. Hence, we visited the terminus of six outlet Glaciers from GrIS and QIC, which are Morris Jesup Glacier, Meehan Glacier, Verhoeff Glacier, Glacier next to Tugto Glacier, Syd Glacier and Hubbard Glacier, to compare the characteristics of the possible growth factors of microorganisms (mineral particle and chemical ions) and microbial diversity. At each site, we collected surface ice samples and bottom sediments at the cryoconite hole for carbon weight, water dissolved ion, characteristics of minerals, counting of microorganisms and DNA analysis.

4.2.3 Kangerlussuaq area

On August 1 and 2, 2013, surface ice collection and measurement of cryoconite hole dimensions were conducted at site RU6 on Russel Glacier in the area of Kangerlussuaq.

5. Summary

We conducted field campaigns in Greenland under the SIGMA Project to elucidate the snow/ice albedo feed-



Fig. 15. Glacial sediment sampling at site SUN1 on Sun Glacier on Jul. 20, 2013.

back effect by snow grain growth and light absorbing snow/ice impurities including glacial microbes on the recent abrupt snow/ice melting in the Arctic. This paper reports the field activities of the field reconnaissance in 2011, the glaciological and meteorological observations by the SIGMA-A&B Party and the biological observations by the Biology Party in 2012–2013 in Greenland.

In 2011, we conducted field reconnaissance in areas of Qaanaaq, Ilulissat and Kangerlussuaq to enable continuous meteorological observations with AWS, glaciological observations and shallow ice core drilling, which were planned to be performed in 2012–2014. Based on the reconnaissance we chose the Qaanaaq area in northwest Greenland as our main activity area and the Kangerlussuaq area in mid-west Greenland partly for biological observations from viewpoints of accessibility, changing tendencies of snow/ice and a balance with existing observation stations and activities.

Our field activities in 2012 were (1) glaciological and meteorological observations together with the installation of two AWSs at sites SIGMA-A on GrIS and SIGMA-B on QIC in June and July (SIGMA-A&B Party) and (2) biological observations on QIC, GrIS and several Glaciers around Qaanaaq from July to August (Biology Party). The SIGMA-A&B Party flew to SIGMA-A by helicopter and stayed there for three weeks from late June to conduct AWS installation, snow pit observation, snow sampling, firn-ice core drilling with a hand auger and meteorological measurements. The meteorological conditions at SIGMA-A were clear and warm in the first half of the period and rain in the second half of the period. During the latter period a record-melting event of surface snow/ice was observed over GrIS. The party also installed an AWS at SIGMA-B on QIC in the middle of July where

the surface was slushy and was covered with snow or ice grains containing dark materials. After installing the AWS at SIGMA-B, a remarkable surface lowering of 53 cm was observed until the middle of August. At the Qaanaaq Geophysical Observatory of DMI, an all-sky camera was installed to monitor the sky condition throughout the year.

In 2012, the Biology Party conducted field investigations on the QIC, Tugto Glacier, which is a small ice cap located in north of Qaanaaq, and on Russel Glacier in the Kangerlussuaq area. Surface snow/ice samples were collected to analyze carbon weight, water dissolved ion, isotopes of minerals, microbial community and DNA sequences. It was found that the carbon amount on the surface ice were higher at QA3 and QA4 as compared to that at other sites (QA1, QA2 and QA-red), indicating that cryoconite granules developed well in the area. A simple AWS was installed at QA3 to monitor air and ice surface temperatures, downward and upward solar radiation (albedo), and ice surface condition by an interval camera. These data will be used to develop a glacial microbe model to simulate the temporal change of surface albedo as functions of growth conditions such as photosynthesis active radiation, temperature and nutrient concentrations.

In 2013, the Biology Party stayed at Qaanaaq (partly in Kangerlussuaq) from the end of June to the beginning of August 2013 for long-term monitoring of glacial microbes on QIC and their effects on albedo. The SIGMA-A&B Party stayed at Qaanaaq and SIGMA-A from the middle of July to the beginning of August 2013. Field observations by the SIGMA-A&B Party in 2013 were basically the same as those in 2012, except for the AWS maintenance. The AWS maintenance at SIGMA-B was conducted in late July, where the surface conditions of QIC were quite different from those during the same period in 2012. Surfaces in large areas at elevations higher than about 700 m were covered with snow. The annual change in snow surface height measured with AWS from September 1, 2012 to the same day in 2013 was +83 cm. Subsequently, the SIGMA-A&B Party flew to SIGMA-A by helicopter and stayed there for one week from the middle of July for AWS maintenance, snow pit observation, snow sampling, firn-ice core drilling with a hand-auger and meteorological measurements. The snow condition of SIGMA-A was dry and quite different from that in the same period of the previous year (highly wet). The annual change in snow surface height from September 1, 2012 to the same day in 2013 was +117 cm. The snow pit observation showed that remarkable snow melting did not occur over the last year at SIGMA-A. Subsequently, the SIGMA-A&B Party flew to SIGMA-A2 by helicopter and performed snow pit observation and drilling of a 6.69-m firn-ice core with a hand auger. The party also conducted AWS maintenance at SIGMA-B, spectral albedo measurements and snow and ice samplings on QIC.

Field observations by the Biology Party in 2013 were conducted mainly in the QIC area, which contains the outlet Glaciers of GrIS and the Glaciers on QIC. Surface ice samples were collected at only QA1 and QA2 due to snow cover at higher elevation sites throughout the summer. Investigations were also conducted on the Sun, Scarlet Heart, Qaqortaq, Sermiarssupaluk and Bowdoin Glaciers, which were accessed by boat, as well as on the Morris Jesup, Meehan, Verhoeff, Syd, Hubbard Glaciers and an unnamed Glacier next to Tugto Glacier, which were accessed by helicopter. On each Glacier, the surface ice and bottom sediments of the cryoconite hole were collected to reveal the spatial variability of the microbial community and the characteristics of the cryoconite. Ice sample collection was also conducted at one site on Russel Glacier in the Kangerlussuaq area.

Acknowledgements

We thank the field campaign members of the SIGMA Project and GRENE-Arctic Project in Greenland in 2012 and 2013. Special thanks are due to Tetsuhide Yamasaki for his dedicated logistic support in 2012 and 2013 and Sakiko Daorana for providing logistics in Qaanaaq. We also thank the helicopter pilots and Ann Jensen of Air Greenland, and Finn Hansen, Hans Jensen, Jesper Olsen, Lars Wille and Ole Mathiesen in Qaanaaq for their logistic support, Svend Erik Ascanius of the Qaanaaq Geophysical Observatory of the Danish Meteorological Institute for supporting the installation of the all-sky camera, and Paul Martin Lund and Merete Laubjerg of Sundhedscsentret in Qaanaaq for the treatment of a frostbitten team member. This study was supported in part by (1) the Japan Society for the Promotion of Science (JSPS), Grant-in-Aid for Scientific Research (S), number 23221004, and (2) the Global Change Observation Mission–Climate (GCOM-C)/the Second-generation GLobal Imager (SGLI) Mission, the Japan Aerospace Exploration Agency (JAXA). The maps shown in Figs. 1, 2 and 4 were created by NunaGIS (<http://en.nunagis.gl/>) operated by Asiaq, Greenland Survey.

References

- Aoki, Te., Aoki, Ta., Fukabori, M., Hachikubo, A., Tachibana, Y. and Nishio, F. (2000): Effects of snow physical parameters on spectral albedo and bidirectional reflectance of snow surface. *J. Geophys. Res.*, **105**, 10,219–10,236, doi: 10.1029/1999JD901122.
- Aoki, T., Hachikubo, A. and Hori, M. (2003): Effects of snow physical parameters on broadband albedos. *J. Geophys. Res.*, **108** (D19), 4616, doi: 10.1029/2003JD003506.
- Aoki, T., Hori, M., Motoyohi, H., Tanikawa, T., Hachikubo, A., Sugiura, K., Yasunari, T. J., Storvold, R., Eide, H. A., Stammes, K., Li, W., Nieke, J., Nakajima, Y. and Takahashi, F. (2007): ADEOS-II/GLI snow/ice products: Part II-Validation results using GLI and MODIS data. *Remote Sens. Environ.*, **111**, 274–290, doi: 10.1016/j.rse.2007.02.035.
- Aoki, T., Kuchiki, K., Niwano, M., Kodama, Y., Hosaka, M. and Tanaka, T. (2011): Physically based snow albedo model for calculating broadband albedos and the solar heating profile

- in snowpack for general circulation models. *J. Geophys. Res.*, **116**, D11114, doi: 10.1029/2010JD015507.
- Aoki, T., Kuchiki, K., Niwano, M., Matoba, S., Uetake, J., Masuda K. and Ishimoto, H. (2013): Numerical Simulation of Spectral Albedos of Glacier Surfaces Covered with Glacial Microbes in Northwestern Greenland, *RADIATION PROCESSES IN THE ATMOSPHERE AND OCEAN (IRS2012)*, Robert Cahalan and Jürgen Fischer (Eds), AIP Conf. Proc. **1531**, 176 (2013); doi: 10.1063/1.4804735.
- Aoki, T., Matoba, S., Yamaguchi, S., Tanikawa, T., Niwano, M., Kuchiki, K., Adachi, K., Uetake, J., Motoyama H. and Hori M. (2014): Light-absorbing snow impurity concentrations measured on Northwest Greenland ice sheet in 2011 and 2012. *Bull. Glaciol. Res.*, **32**, 21–31.
- Box, J. E., Fettweis, X., Stroeve, J. C., Tedesco, M., Hall, D. K. and Steffen, K. (2012): Greenland ice sheet albedo feedback: thermodynamics and atmospheric drivers. *The Cryosphere*, **6**, 821–839, doi: 10.5194/tc-6-821-2012.
- Brun, E., Yang, Z. L., Essery, R. and Cohen, J. (2008): Snow cover parameterization and modeling, in *Snow and Climate*, edited by Armstrong, R. L. and Brun, E., Cambridge Univ. Press, New York, pp. 125–180.
- Carmagnola, C. M., Domine, F., Dumont, M., Wright, P., Strellis, B., Bergin, M., Dibb, J., Picard, G., Libois, Q., Arnaud, L. and Morin, S. (2013): Snow spectral albedo at Summit, Greenland: measurements and numerical simulations based on physical and chemical properties of the snowpack. *The Cryosphere*, **7**, 1139–1160, doi: 10.5194/tc-7-1139-2013.
- Chýlek, P., Srivastava, V., Cahenzli, L., Pinnick, R. G., Dod, R. L., Novakov, T., Cook, T. L. and Hinds, B. D. (1987): Aerosol and graphitic carbon content of snow. *J. Geophys. Res.*, **92**, 9801–9809.
- Chýlek, P., Johnson, B., Damiano, P. A., Taylor, K. C. and Clement, P. (1995): Biomass burning record and black carbon in the GISP2 Ice Core. *Geophys. Res. Lett.*, **22**, 89–92.
- Clarke, A. D. and Noone, K. J. (1985): Soot in the arctic snowpack: A cause for perturbations in radiative transfer. *Atmos. Environ.*, **19**, 2045–2053.
- Doherty, S. J., Warren, S. G., Grenfell T. C., Clarke, A. D. and Brandt, R. E. (2010): Light-absorbing impurities in Arctic snow. *Atmos. Chem. Phys.*, **10**, 18807–18878, doi: 10.5194/acp-10-11647-2010, 11647–11680.
- Doherty, S. J., Grenfell, T. C., Forsström, S., Hegg, D. L., Brandt, R. E. and Warren, S. G. (2013): Observed vertical redistribution of black carbon and other insoluble light-absorbing particles in melting snow. *J. Geophys. Res.*, **118**, 5553–5569, doi: 10.1002/jgrd.50235.
- Fettweis, X., Franco, B., Tedesco, M., van Angelen, J. H., Lenaerts, J. T. M., van den Broeke, M. R. and Gallee, H. (2013): Estimating Greenland ice sheet surface mass balance contribution to future sea level rise using the regional atmospheric model MAR. *The Cryosphere*, **7**, 469–489, doi: 10.5194/tc-7-469-2013.
- Fierz, C., Armstrong, R. L., Durand, Y., Etchevers, P., Greene, E., McClung, D. M., Nishimura, K., Satyawali P. K. and Sokratov, S. A. (2009): *The international classification for seasonal snow on the ground*. IHP-VII Technical Documents in Hydrology No. **83**, IACS Contribution No.1, UNESCO-IHP, Paris, 90 pp.
- Flanner, M. G., Zender, C. S., Randerson, J. T. and Rasch, P. J. (2007): Present-day Climate forcing and response from black carbon in snow. *J. Geophys. Res.*, **112**, D11202, doi: 10.1029/2006JD008003.
- Flanner, M. G., Zender, C. S., Hess, P. G., Mahowald, N. M., Painter, T. H., Ramanathan V. and Rasch, P. J. (2009): Springtime warming and reduced snow cover from carbonaceous particles. *Atmos. Chem. Phys.*, **9**, 2481–2497.
- Hagler, G. S. W., Bergin, M. H., Smith, E. A., Dibb, J. E., Anderson, C. and Steig, E. J. (2007): Particulate and water-soluble carbon measured in recent snow at Summit, Greenland. *Geophys. Res. Lett.*, **34**, L16505, doi: 10.1029/2007GL030110.
- Hansen, J. and Nazarenko, L. (2004): Soot Climate forcing via snow and ice albedos. *Proc. Natl. Acad. Sci. U.S.A.*, **101**, 423–428.
- Hori, M., Aoki, T., Stamnes, K. and Li, W. (2007): ADEOS-II/GLI snow/ice products - part III: Retrieved results. *Remote Sens. Environ.*, **111**, 274–319, doi: 10.1016/j.rse.2007.01.025.
- McConnell, J. R., Edwards, R., Kok, G. L., Flanner, M. G., Bender, C. S., Saltzman, E. S., Banta, J. R., Pasteris, D. R., Carter, M. M. and Kahl, J. D. W. (2007): 20th-century industrial black carbon emissions altered arctic Climate forcing. *Science*, **317**, 1381, doi: 10.1126/science.1144856.
- Ministry of Education, Culture, Sports, Science and Technology Japan (MEXT), (2012): "Green Network of Excellence" (GRENE) Program, *Arctic Climate Change Research Project Rapid Change of the Arctic Climate System and its Global Influences 2011–2016*, (available from http://www.nipr.ac.jp/grene/e/grene_E.pdf), 12pp.
- Nghiem, S. V., Hall, D. K., Mote, T. L., Tedesco, M., Albert, M. R., Keegan, K., Shuman, C. A., DiGirolamo, N. E. and Neumann, G. (2012): The extreme melt across The Greenland ice sheet in 2012. *Geophys. Res. Lett.*, **39**, L20502, doi: 10.1029/2012GL053611.
- Niwano, M., Aoki, T., Kuchiki, K., Hosaka, M. and Kodama, Y. (2012): Snow Metamorphism and Albedo Process (SMAP) model for Climate studies: Model validation using meteorological and snow Impurity data measured at Sapporo, Japan. *J. Geophys. Res.*, **117**, F03008, doi: 10.1029/2011JF002239.
- Palmer, J. (2012): From ice to water-watching Greenland melt. *Sphere*, **23**, CIRES, University of Colorado Boulder and NOAA, 22–23.
- Pedersen, C. A. and Winther, J. G. (2005): Intercomparison and validation of snow albedo parameterization schemes in Climate models. *Climate Dyn.*, **25**, 351–362.
- Rae, J. G. L., Aðalgeirsdóttir, G., Edwards, T. L., Fettweis, X., Gregory, J. M., Hewitt, H. T., Lowe, J. A., Lucas-Picher, P., Mottram, R. H., Payne, A. J., Ridley, J. K., Shannon, S. R., van de Berg, W. J., van de Wal, R. S. W., and van den Broeke, M. R. (2012): Greenland ice sheet surface mass balance: evaluating simulations and making projections with regional Climate models, *The Cryosphere*, **6**, 1275–1294, doi:10.5194/tc-6-1275-2012.
- Rignot, E., Velicogna, I., van den Broeke, M. R., Monaghan, A. and Lenaerts, J. (2011): Acceleration of the contribution of The Greenland and Antarctic ice sheets to sea level rise. *Geophys. Res. Lett.*, **38**, L05503, doi: 10.1029/2011GL046583.
- Sørensen, L. S., Simonsen, S. B., Nielsen, K., Lucas-Picher, P., Spada, G., Adalgeirsdottir, G., Forsberg, R. and Hvidberg, C. S. (2011): Mass balance of The Greenland ice sheet (2003–2008) from ICESat data—the impact of interpolation, sampling and firn density, *The Cryosphere*, **5**, 173–186, doi: 10.5194/tc-5-173-2011.
- Stamnes, K., Li, W., Eide, H., Aoki, T., Hori, M. and Storvold, R. (2007): ADEOS-II/GLI snow/ice products-part I: Scientific Basis. *Remote Sens. Environ.*, **111**, 258–273, doi: 10.1016/j.rse.2007.03.023.
- Steffen, K. and Box, J. E. (2001): Surface climatology of The Greenland ice sheet: Greenland Climate network 1995–1999. *J. Geophys. Res.*, **106** (D24), 33,951–33,964, doi: 10.1029/2001JD900161.
- Steffen, K., Clark, P. U., Cogley, J. G., Holland, D., Marshall, S., Rignot, E. and Thomas, R. (2008): Chapter 2. *Rapid changes in Glaciers and ice sheets and their impacts on sea level in “Abrupt Climate Change Science Program and the Subcommittee on Global Change Research”*, 60–142 (US Geological Survey).
- Stibal, M., Telling, J., Cook, J., Mak, K. M., Hodson, A. and Anesio, A. M. (2012): Environmental controls on microbial abundance and activity on The Greenland ice sheet: a multivariate analysis approach. *Microbalecology*, **63** (1), 74–84.
- Sugiyama, S., Sakakibara, D., Matsuno, S., Yamaguchi, S., Matoba S. and Aoki, T. (2014): Initial field observations on Qaanaaq ice cap in northwestern Greenland. *Ann. Glaciol.*, **55**, 25–33, doi: 10.3189/2013AoG66A102.

- Takeuchi, N. (2002): The surface albedo and characteristics of cryoconite (biogenic surface dust) on the Gulkana Glacier in Alaska. *Bull. Glaciol. Res.*, **19**, 63–70.
- Takeuchi, N., Matsuda, Y., Sakai, A. and Fujita, K. (2005). A large amount of biogenic surface dust (cryoconite) on a Glacier in the Qilian Mountains, China. *Bull. Glaciol. Res.*, **22**, 1–8.
- Tedesco, M., Fettweis, X., Mote, T., Wahr, J., Alexander, P., Box, J. E. and Wouters, B. (2013): Evidence and analysis of 2012 Greenland records from spaceborne observations, a regional Climate model and reanalysis data. *The Cryosphere*, **7**, 615–630, doi: 10.5194/tc-7-615-2013.
- Uetake, J., Naganuma, T., Hebsgaard, M. B., Kanda, H. and Kohshima, S. (2010): Communities of algae and cyanobacteria on Glaciers in west Greenland. *Polar Science*, **4**, 71–80, doi: 10.1016/j.polar.2010.03.002.
- van As, D., Fausto, R. S. and the PROMICE project team (2011): Programme for Monitoring of The Greenland Ice Sheet (PROMICE): first temperature and ablation records. *Geological Survey of Denmark and Greenland Bulletin*, **23**, 73–76.
- van den Broeke, M., Smeets, P., Ettema, J., van der Veen, C., van de Wal, R. and Oerlemans, J. (2008): Partitioning of melt energy and meltwater fluxes in the ablation zone of the west Greenland ice sheet. *The Cryosphere*, **2**, 179–189, doi: 10.5194/tc-2-179-2008.
- van den Broeke, M., Bamber, J., Ettema, J., Rignot, E., Schrama, E., van de Berg, W. J., van Meijgaard, E., Velicogna, I. and Wouters, B. (2009): Partitioning recent Greenland mass loss. *Science*, **326**, 984–986, doi: 10.1126/science.1178176.
- van den Broeke, M. R., Smeets, C. J. P. P. and van de Wal, R. S.W. (2011): The seasonal cycle and interannual variability of surface energy balance and melt in the ablation zone of the west Greenland ice sheet. *The Cryosphere*, **5**, 377–390, doi: 10.5194/tc-5-377-2011.
- Warren, S. G. and Wiscombe, W. J. (1980): A model for the spectral albedo of snow, II: Snow containing atmospheric aerosols. *J. Atmos. Sci.*, **37**, 2734–2745.
- Wientjes, I. G. M., Van de Wal, R. S. W., Reichart, G. J., Sluijs, A. and Oerlemans, J. (2011): Dust from the dark region in the western ablation zone of The Greenland ice sheet. *The Cryosphere*, **5**, 589–601, doi: 10.5194/tc-5-589-2011.
- Wientjes, I. G. M., De Van Wal, R. S. W., Schwikowski, M., Zapf, A., Fahrni, S. and Wacker, L. (2012). Carbonaceous particles reveal that Late Holocene dust causes the dark region in the western ablation zone of The Greenland ice sheet. *J. Glaciol.*, **58**, 787–794, doi: 10.3189/2012JoG11J165.
- Wiscombe, W. J. and Warren, S. G. (1980): A model for the spectral albedo of snow, I: Pure snow. *J. Atmos. Sci.*, **37**, 2712–2733.
- Yallop, M. L., Anesio, A. M., Perkins, R. G., Cook, J., Telling, J., Fagan, D., MacFarlane, J., Stibal, M., Barker, G., Bellas, C., Hodson, A., Tranter, M., Whadhan, J. and Roberts, N. W. (2012). Photophysiology and albedo-changing potential of the ice algal community on the surface of The Greenland ice sheet. *The ISME Journal*, **6** (12), 2302–2313, doi: 10.1038/ismej.2012.10.